AF469010) was obtained by probing a honey bee brain cDNA library with the positive PCR fragment. Overall similarity to *Drosophila for* (*dg2*), 87%; *Drosophila dg1*, 70%; mammalian *pkg1*, 73%; *Caenorhabditis elegans pkg*, 70%.

6. Each Northern blot lane contained 5 μg of mRNA from heads. Hybridization was performed with a 742–base pair DIG-labeled riboprobe (corresponding to nucleotides 1561 to 2302 of *Amfor*), using EasyHyb buffer (Roche) at 65°C. *Ef1α* loading control was as in (*23*).
7. To measure mRNA levels of *Amfor* in individual bee brains, we used real-time qRT-PCR with TaqMan technology (ABI). Total brain RNA from an individual brain was isolated with the RNeasy mini kit (Qiagen). Reverse transcription was performed according to protocol (TaqMan Reverse Transcription Reagents kit, ABI) with 100 ng of total RNA. PCR was performed with the default parameters of the ABI Prism 5700 sequence detector. PrimerExpress software (ABI) was used to design highly specific primers and probe for *Amfor*. Forward probe, 5′-AATATAACTTCCGGTGCAACGTATT; reverse probe, 5′-CGTTTGGATCACGGAAGAAAG; TaqMan probe (ABI), 5′-FAM6-AGGCGTGCCGCAGAAGGTCCA-TAMRA. Levels of *Amfor* were quantified relative to 18*S* rRNA (ABI kit); there were no differences in 18*S* rRNA levels between nurses and foragers (*11*). Each sample was analyzed in triplicate, and each data point was calculated as the average of the three. Quantification was based on the number of PCR cycles (Ct) required to cross a threshold of fluorescence intensity, using the $2^{-\Delta\Delta Ct}$ technique (ABI User Bulletin 2) described in (*24*). Identification of nurses and foragers was as in (*25*). Bees were collected into liquid nitrogen immediately upon identification so that mRNA measurements accurately reflected gene activity under natural conditions. Bees were stored at −80°C until brain dissection.
8. One-day-old (0 to 24 hours) adult bees were obtained by removing honeycomb frames containing pupae from a typical colony in the field and transferring them to an incubator (33°C, 95% relative humidity). We marked ~1000 1-day-old bees with a paint spot on their thorax and placed them in a small beehive with a queen (unrelated to the workers), one honeycomb frame of honey and pollen, and one empty honeycomb frame (for the queen to lay eggs). Each single-cohort colony was placed in an incubator for the first 4 days and then moved outdoors.
9. Z. Y. Huang, G. E. Robinson, *Proc. Natl. Acad. Sci. U.S.A.* **89**, 11726 (1992).
10. We marked groups of 50 1-day-old bees and placed each group in a wooden cage (6 cm by 12 cm by 18 cm) placed in an incubator (33°C, 95% relative humidity) for 4 days. Bees were treated orally with a 50% sucrose solution containing 8-Br-cGMP (Sigma) at the specified dose (control bees received sucrose alone). This compound is known to increase PKG activity (*26*). A freshly mixed solution was given daily. On day 5, all surviving bees from each cage were counted (90 to 100% survival) and placed into a single-cohort colony with ~1000 1-day-old bees (without cGMP treatment). Observations at the hive entrance were made as in (*9*) to ensure that the onset of foraging was identified; observations then occurred for 4 hours per day, 2 hours in the morning and 2 hours in late afternoon—times of peak foraging activity for these colonies. All bees initiating foraging during the first 4 days of observation were marked with a second spot of paint (so they were counted just once) and recorded, and the cumulative percentage of each group that foraged precociously was calculated. Oral treatment was used because it is a noninvasive way of achieving chronic treatment; it does not allow effects to be conclusively ascribed to brain elevation, even though assays of PKG activity in the head suggest that elevation in the brain did occur.
11. Y. Ben-Shahar, A. Robichon, M. B. Sokolowski, G. E. Robinson, data not shown.
12. Brains were dissected fresh in saline. Bees were cold-anesthetized before dissection. Once dissected, brains were immediately freeze-mounted on dry ice with anterior side (identified by antennal lobes) up, and transferred to the cryostat (Bright Inst. Co., −20°C). Brains were sectioned (10 μm) and dry-mounted on glass slides. Hybridization was performed in 50% formaldehyde buffer with a digoxigenin-labeled antisense RNA probe (Roche) at 60°C [same as in (*6*)]. Sense probe was used as control.
13. M. Heisenberg, *Learn. Mem.* **5**, 1 (1998).
14. W. Gronenberg, *J. Comp. Neurol.* **435**, 474 (2001).
15. R. E. Page Jr., J. Gadau, M. Beye, *Genetics* **160**, 375 (2002).
16. L. J. Young, M. M. Lim, B. Gingrich, T. R. Insel, *Horm. Behav.* **40**, 133 (2001).
17. M. J. B. Krieger, K. G. Ross, *Science* **295**, 328 (2002).
18. M. A. Della-Fera, C. A. Baile, S. R. Peikin, *Physiol. Behav.* **26**, 799 (1981).
19. J. E. Morley, S. A. Farr, M. D. Suarez, J. F. Flood, *Pharmacol. Biochem. Behav.* **50**, 369 (1995).
20. L. L. Moroz, T. P. Norekian, T. J. Pirtle, K. J. Robertson, R. A. Satterlie, *J. Comp. Neurol.* **427**, 274 (2000).
21. Y. Gilad, S. Rosenberg, M. Przeworski, D. Lancet, K. Skorecki, *Proc. Natl. Acad. Sci. U.S.A.* **99**, 862 (2002).
22. Y.-C. Ding *et al.*, *Proc. Natl. Acad. Sci. U.S.A.* **99**, 309 (2002).
23. D. P. Toma *et al.*, *Proc. Natl. Acad. Sci. U.S.A.* **97**, 6914 (2000).
24. G. Bloch *et al.*, *J. Biol. Rhythms* **16**, 444 (2001).
25. Y. Ben-Shahar, G. E. Robinson, *J. Comp. Physiol. A* **187**, 891 (2001).
26. S. H. Francis *et al.*, *Mol. Pharmacol.* **34**, 506 (1988).
27. E. O. Wilson, *Sociobiology* (Belknap/Harvard, Cambridge, MA, 1975).
28. D. R. Cox, *J. R. Stat. Soc. Ser. B* **34**, 187 (1995).
29. We thank B. White for use of the ABI 5700 TaqMan machine; A. Ross and A. Cash for technical assistance in the field; S. Hartz for statistical assistance; S. E. Fahrbach and R. Velarde for help with in situ hybridization; and D. F. Clayton, K. G. Ross, J. H. Willis, and members of the Robinson and Sokolowski laboratories for helpful comments on the manuscript. The "time scale perspective" on genomic responsiveness resembles Wilson's model for organismic responsiveness (*27*). Supported by grants from the NIH and Burroughs-Wellcome Trust (G.E.R.) and MRC and the Canada Research Chair Program (M.B.S.).

16 January 2002; accepted 20 March 2002

# A Tomato Cysteine Protease Required for *Cf-2*–Dependent Disease Resistance and Suppression of Autonecrosis

**Julia Krüger,[1] Colwyn M. Thomas,[1,2] Catherine Golstein,[1,3] Mark S. Dixon,[1,4] Matthew Smoker,[1] Saijun Tang,[1,5] Lonneke Mulder,[1] Jonathan D. G. Jones[1]***

**Little is known of how plant disease resistance (R) proteins recognize pathogens and activate plant defenses. *Rcr3* is specifically required for the function of *Cf-2*, a *Lycopersicon pimpinellifolium* gene bred into cultivated tomato (*Lycopersicon esculentum*) for resistance to *Cladosporium fulvum*. *Rcr3* encodes a secreted papain-like cysteine endoprotease. Genetic analysis shows *Rcr3* is allelic to the *L. pimpinellifolium Ne* gene, which suppresses the *Cf-2*–dependent autonecrosis conditioned by its *L. esculentum* allele, *ne* (*necrosis*). *Rcr3* alleles from these two species encode proteins that differ by only seven amino acids. Possible roles of Rcr3 in Cf-2–dependent defense and autonecrosis are discussed.**

Plant disease R proteins activate defense mechanisms upon perception of pathogen-derived molecules. Intracellular and extracellular race-specific elicitors are recognized by structurally distinct classes of R proteins (*1*, *2*). Tomato *Cf*-genes confer resistance to the fungus *Cladosporium fulvum*. During infection numerous peptides are secreted into the apoplast (*3*), and some are products of fungal avirulence (*Avr*) genes. *Cf*- genes encode transmembrane proteins with extracellular leucine-rich repeats (LRRs) and short (23 to 36 amino acid) cytoplasmic domains (*1*, *2*). In tomato, Avr peptide recognition activates a defense reaction dependent on *Cf*- genes, the hypersensitive response (HR), which results in localized cell death and the arrest of pathogen ingress. In tobacco cells expressing *Cf-9*, elicitation with Avr9 leads within 5 to 15 min to reactive oxygen production, protein kinase activation and novel gene expression (*4*). How Cf proteins activate defense responses is unknown.

*Cf-2* confers *Avr2*-dependent resistance to *C. fulvum*. Mutations in *Rcr3* suppress *Cf-2* function (*2*). *Rcr3* is unlikely to be a component shared by multiple *Cf*- signaling pathways, because it is dispensable for the function of *Cf-9* and even *Cf-5*, an ortholog of *Cf-2* (*5*).

We isolated *Rcr3* by positional cloning (*6*). *Rcr3* encodes a protein of 344 amino acids that is 43% identical to papain from *Carica papaya* (Fig. 1A). *Rcr3* expressed from its own promoter restores *Cf-2*–dependent resistance to *rcr3* mutants (Fig. 1B). Rcr3 contains conserved amino acid residues of the active site of eukaryotic thiol proteases ($C^{154}$, $H^{286}$, and $N^{307}$ (*7*),

[1]The Sainsbury Laboratory, John Innes Centre, Norwich NR4 7UH, UK. [2]School of Biological Sciences, University of East Anglia, Norwich NR4 7TJ, UK. [3]Department of Biology, Indiana University, Bloomington, IN 47405, USA. [4]School of Biological Sciences, University of Southampton, Southampton SO16 7PX, UK. [5]Department of Biology, 108 Coker Hall, University of North Carolina, Chapel Hill, NC 27599–3280, USA.

*To whom correspondence should be addressed. E-mail jonathan.jones@bbsrc.ac.uk

Fig. 1A), and six cysteines that form three putative cystine bridges. Single nucleotide exchanges were found in all *rcr3* mutants (*6*) resulting in single amino acid exchanges in *rcr3-1* and *rcr3-2*, and premature translation stop codons in *rcr3-3* and *rcr3-4* (Fig. 1A). The *rcr3-1* mutation, a C to S substitution at position 151 ($C^{151}S$), does not completely compromise *Cf-2* function (*2*), and serine is found at a similar position in other cysteine proteases (PROSITE: PDOC00126). The $G^{314}V$ substitution in *rcr3-2* results in complete loss of function.

*Rcr3* expression is regulated developmentally and in response to *C. fulvum* infection. *Rcr3* mRNA levels are elevated in older plants irrespective of leaf age (Fig. 1C). After infection with *C. fulvum*, *Rcr3* expression is elevated in compatible (disease causing) interactions, but much more rapidly in incompatible (resistant) interactions mediated by *Cf-2* or *Cf-9* (Fig. 1C). The regulation of *Rcr3* expression resembles that of pathogenesis-related genes (*8*).

We sequenced *Rcr3* in several *Lycopersicon* species and in *L. esculentum* near-isogenic lines. Analysis of *Rcr3* from *L. pimpinellifolium* ($Rcr3^{pim}$) revealed nucleotide changes leading to a deletion of one amino acid and six amino acid exchanges compared with the *L. esculentum* allele ($Rcr3^{esc}$; Fig. 1A). The Cf2 line contains $Rcr3^{pim}$ (Fig. 1A), suggesting it was cointrogressed with *Cf-2* even though the genes are unlinked (*2*). Another breeding line containing *Cf-2* (Ontario 7620) also contains $Rcr3^{pim}$. During introgression of *Cf-2* into tomato, a second *L. pimpinellifolium* gene (*Ne*) was required to suppress *Cf-2*–dependent autonecrosis conditioned by its *L. esculentum* allele (*ne*, *necrosis*) (*9*). The $F_2$ progeny from a *L. esculentum* × *L. pimpinellifolium* (*Cf-2*) cross, which carry *Cf-2* and are homozygous for *ne,* are autonecrotic. This phenotype first appears in older leaves after the onset of flowering but eventually spreads to all leaves.

We investigated whether $Rcr3^{pim}$ and *Ne* are allelic by testing if *rcr3* mutants had lost *Ne* function. When Cf2 rcr3-2 and Cf0 (*ne/ne*) lines were crossed, the $F_1$ progeny showed necrotic lesions on older leaves comparable to those observed in *Cf-2/+*, *ne/ne* plants (Fig. 2A). Therefore, mutations in $Rcr3^{pim}$ abolish *Ne* function. The phenotypes of Cf2 rcr3-3 transgenic plants transformed with the clone p28L2 (*10*) that contains $Rcr3^{esc}$ were also analyzed, and those plants that exhibited *Cf-2*–dependent resistance to *C. fulvum* infection also developed autonecrotic lesions (Fig. 2A). Thus, $Rcr3^{esc}$ actively confers *Cf-2*–dependent necrosis. We also characterized two *Cf-9/Cf-2* chimeras (*11*). In the *pCf-9:Cf-2* chimera, *Cf-2* is expressed from the *Cf-9* promoter (Fig. 2B). The *Cf-2/9* chimera encodes a protein with the 34 $NH_2$-terminal LRRs of Cf-2 fused to three COOH-terminal LRRs and COOH-terminal sequences of Cf-9, expressed from the *Cf-2* promoter (Fig. 2B). Both chimeras confer *Avr2*- and *Rcr3*-dependent resistance to *C. fulvum* infection (*12*). Because the resistance conferred by *Cf-2/9* requires *Rcr3*, when *Cf-9* does not (*2*), this requirement must be a property of the extracellular LRR domain of Cf-2.

Cf0 plants expressing a *Cf-2* transgene (*13*) or the *Cf-2/9* chimera are not autonecrotic. Therefore, *Cf-2* expression may be necessary but not always sufficient for autonecrosis. However, $Rcr3^{esc}$-dependent autonecrosis was observed in Cf0 transgenic plants expressing *pCf-9:Cf-2* (*14*) (Fig. 2D). The *Cf-9* promoter is stronger than that of *Cf-2* (*15*). In older tomato plants, increased levels of *Rcr3* mRNA are observed (Fig. 1C). Elevated expression of pathway components may inappropriately activate *Cf-2*–dependent plant defenses. Together these data demonstrate that *Rcr3* is required for *Cf-2*–dependent resistance to *C. fulvum* infection, and that $Rcr3^{pim}$ (*Ne*) can suppress $Rcr3^{esc}$(*ne*)-dependent autonecrosis.

The papain class of cysteine proteases is translated into a prepro form, with a signal peptide for localization to the vacuole or extracellular space and a prodomain that blocks the active site until proteolytic removal (*16*). To localize Rcr3 and to assay protease activity, *Rcr3* was expressed transiently in *Nicotiana benthamiana* (*17*). Leaves were infiltrated with *Agrobacterium tumefaciens* carrying a 35*S*:histidine (His)- and hemagglutinin (HA)-tagged *Rcr3* fusion. A protein of

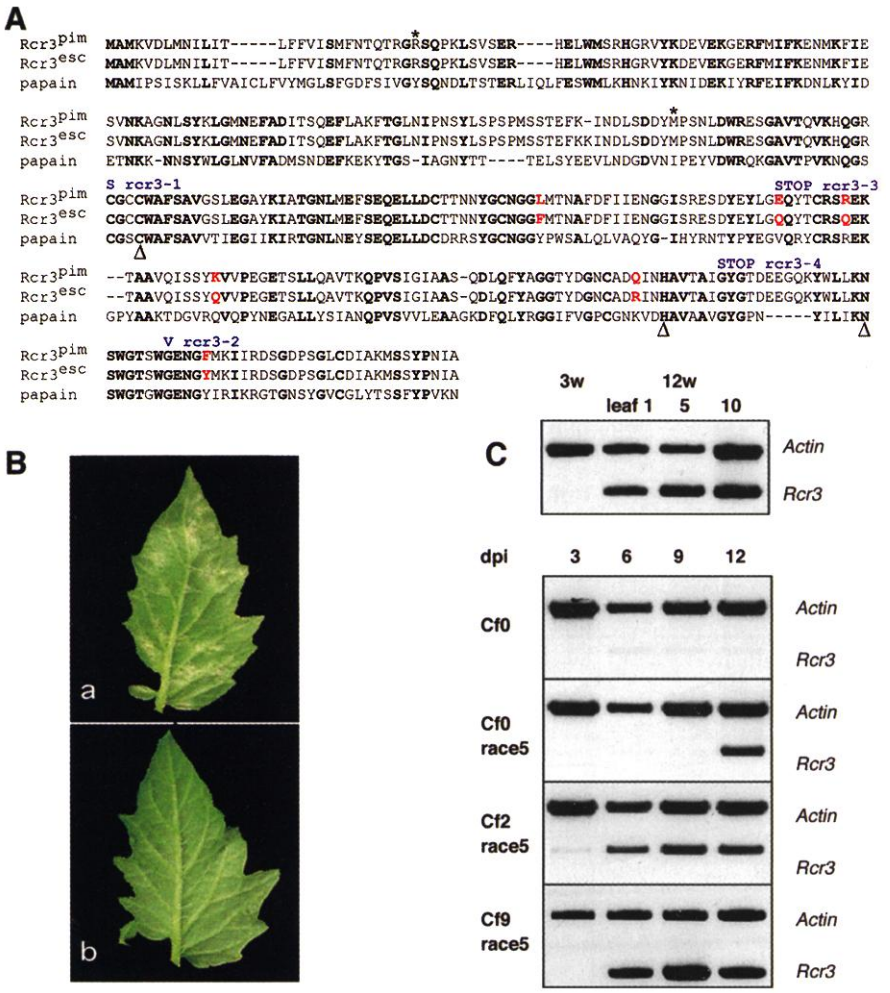


**Fig. 1.** Rcr3 characterization. (**A**) Alignment of Rcr3 from *L. pimpinellifolium* ($Rcr3^{pim}$), *L. esculentum* ($Rcr^{esc}$), and papain. Identical amino acids are shown in bold, allele-specific differences in red, and rcr3 mutant residues in blue. Asterisks indicate the first amino acid after the predicted signal peptide and prodomain cleavage sites, and triangles indicate the protease catalytic residues. (**B**) Complementation of Cf2 rcr3-3 mutants with *pRcr3:Rcr3*$^{pim}$. The abaxial surface of tomato leaves is shown 16 days after infection with *C. fulvum* race 5 that expresses *Avr2*. (a) Disease-sensitive Cf2 rcr3-3 control; (b) Cf2 rcr3-3 transformed with *pRcr3:Rcr3*. (**C**) Expression of *Rcr3*. Upper panel, reverse-transcriptase–polymerase chain reaction (RT-PCR) products of *Rcr3* and *actin* as a control for RNA prepared from Cf2 plants of different ages. Lane 1, 3-week-old plant, lanes 2 to 4, 12-week-old plant, RNA was prepared from the leaf indicated. Lower panel, RT-PCR products of *Rcr3* and *actin* in 2-week-old plants inoculated with *C. fulvum* race 5 in compatible (Cf0) or incompatible interactions (Cf2, Cf9) at 3, 6, 9, and 12 days postinfection (dpi).

the predicted size for the secreted, unprocessed Rcr3 (38 kD) was observed in total extracts using the HA antibody (Fig. 3B). In the apoplastic intercellular fluid (*18*), a second band that corresponds to the predicted size of Rcr3 lacking its prodomain was detected (Fig. 3B).

These smaller forms of Rcr3-His and Rcr3-His-HA proteins were affinity-purified from intercellular fluid using TALON beads (Clontech) (*6*) and tested for protease activity in gels containing gelatin (*19*). A zone of clearing was detected within the gel due to gelatin degradation. This zone was specific for intercellular fluid containing epitope-tagged Rcr3 and was also detected in the TALON eluate (Fig. 3C). Thus, mature Rcr3 can utilize gelatin as a substrate. We also used a protease assay that detects cleavage of fluorescein thiocarbamoyl (FTC)– labeled casein (Fig. 3D). Protease activity in intercellular fluid was partially inhibited and, in affinity-purified preparations, was almost completely inhibited by E-64, a specific inhibitor of papainlike cysteine proteases (*20*).

We show here that Rcr3 is a positive regulator of *Cf-2*–dependent resistance and that *Rcr3*$^{esc}$ is also a positive regulator of *Cf-2*–dependent autonecrosis. The molecular mechanism for *Rcr3*$^{pim}$ suppression of *Rcr3*$^{esc}$-dependent autonecrosis remains to be determined. Because Rcr3 is a secreted cysteine protease and it has a specific role in *Cf-2*–mediated resistance, it likely functions upstream of Cf-2.

Plant proteases are involved in a multitude of cellular processes (*21–23*). Several roles for a protease in *Cf-2*–dependent resistance can be envisaged. Rcr3 might process Avr2 to generate a mature ligand. Several *C. fulvum* avirulence proteins, including Avr4 and Avr9, are proteolytically processed in planta (*3*). Processing of a peptide ligand is exemplified by the generation

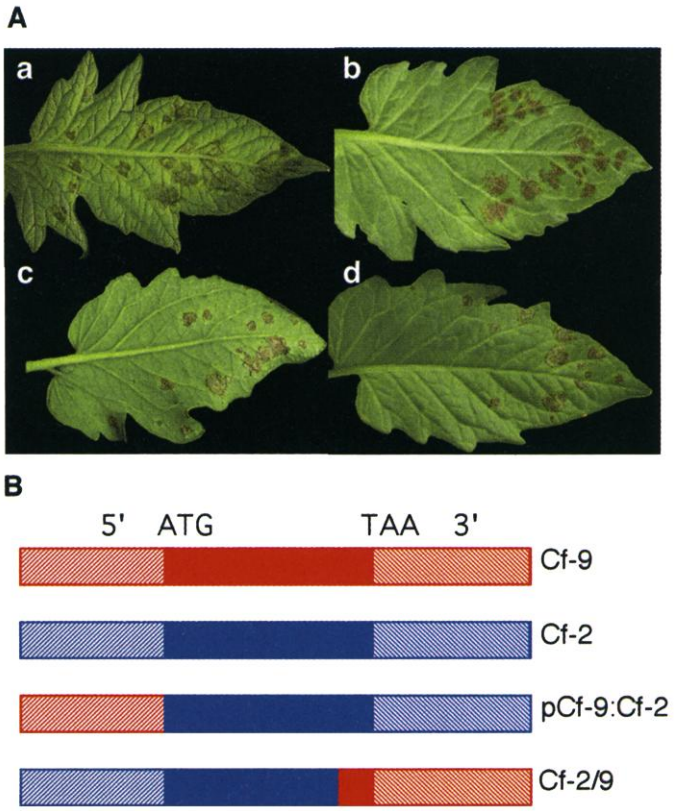


**Fig. 2.** *Rcr3*$^{pim}$ is *Ne*, *Rcr3*$^{esc}$ is *ne*. (**A**) Autonecrosis is *Rcr3*$^{esc}$-dependent. Leaflets of 12-week-old plants with the following genotypes; (a) *Cf-2/+*, *ne/ne*; (b) Cf0 × Cf2 rcr3-3 $F_1$; (c) Cf2 rcr3-3 expressing the *Rcr3*$^{esc}$ transgene on p28L2; (d) transgenic Cf0 expressing *pCf-9: Cf-2*. (**B**) Schematic representation of *Cf-9*, *Cf-2*, and two chimeras. Fragments of genomic clones of *Cf-9* and *Cf-2* were exchanged (*11*). 5′ signifies 5′ flanking DNA; 3′ signifies 3′ flanking DNA. *Cf-2/9* contains 5′ coding sequences from *Cf-2* fused to the 3′ coding region of *Cf-9*. In *pCf-9:Cf-2*, *Cf-2* is expressed from the *Cf-9* promoter.

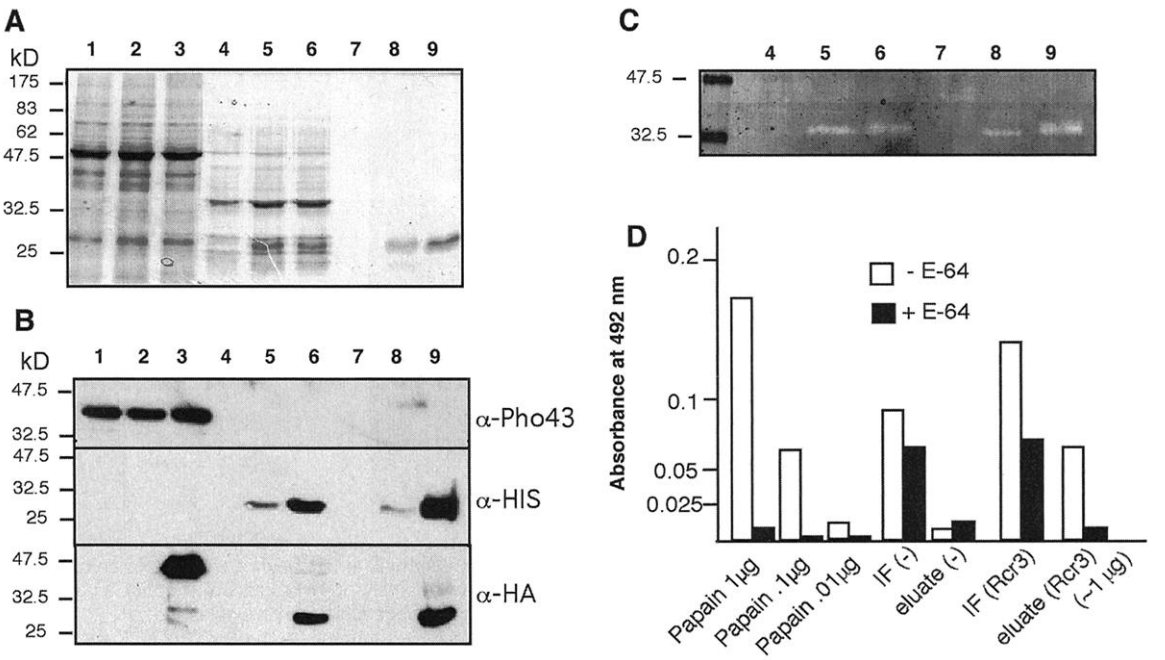


**Fig. 3.** Rcr3 is a secreted protease. (**A**) Coomassie blue–stained gel of *N. benthamiana* total cellular protein, intercellular fluid (IF) protein and affinity-purified Rcr3. Lanes 1 to 3 were loaded with total plant extracts, lanes 4 to 6 with IF and lanes 7 to 9 with the eluate from a TALON column. Lanes 1, 4, and 7 show proteins from plants expressing empty vector control; lanes 2, 5, and 8 show proteins from plants expressing pMWBin19Rcr3:His and lanes 3, 6, and 9 show proteins from plants expressing pMWBin19Rcr3:His:HA. (**B**) Western blots of samples shown above were probed with the antibodies as indicated on the right of the panels. (**C**) Lane numbers correspond to samples shown above. In-gel assay of total IF and affinity-purified proteins using gelatin as substrate detects protease activity at approximately 34 kD under these conditions. (**D**) Protease assay using FTC-casein as substrate. Incubation was for 16 hours at 30°C in the presence (black columns) or absence (white columns) of 5 μM E-64, a cysteine protease inhibitor. Total intercellular fluid and affinity-purified proteins (eluate) from plants expressing empty vector (–) or pMWBin19Rcr3:His:HA (Rcr3).

of the spätzle ligand for the *Drosophila* Toll receptor that is generated via a serine protease cascade (*24*). In mature flies, Toll also functions in immunity to fungal pathogens, and derepression of this pathway, due to the absence of the Spn43Ac protease inhibitor, also results in necrosis (*25*).

Generating a mature ligand is unlikely to be the sole function of Rcr3, because *rcr3* mutants do not exhibit an HR when infiltrated with intercellular fluid preparations that contain Avr2 isolated from infected tomato plants (*2*).

Alternatively, Rcr3 could process Cf-2 or another plant protein. Differences in the substrate specificity or activity of $Rcr3^{pim}$ and $Rcr3^{esc}$ might explain why $Rcr3^{esc}$ induces Avr2-independent necrosis. An extracellular protease is also required for brassinosteroid perception in *Arabidopsis* (*26*). Overexpression of the serine carboxypeptidase BRS1 suppresses extracellular domain mutants of the BRI1 LRR-receptor kinase. BRS1 may process a protein that forms part of the BRI1 ligand (*26*). Alternatively, Rcr3 might be a plant defense component that is inhibited by Avr2. Avr2 could also inhibit other cysteine proteases, either by binding to or by modifying them. Whether Rcr3 has a role in defense is not established. The Cf2 Rcr3 mutant lines do not appear more susceptible to *C. fulvum* than Cf0, but tomato encodes many different cysteine proteases. It is interesting that the *C. fulvum* Avr9 protein shows significant structural homology to several protease inhibitors (*27*).

It is possible that Avr2 and Rcr3 together constitute a complex ligand that is recognized by Cf-2. It has been suggested that R proteins act as 'guards' for specific proteins targeted by pathogen Avr proteins during infection (*1*, *2*). Cf-2 may guard Rcr3 and trigger a defense response upon perception of an Rcr3/Avr2 complex. In *rcr3* mutants, no Avr2-independent signaling would occur either because no $Rcr3^{pim}$/Cf-2 complex is formed or because the complex does not activate defense signaling. A subtle structural difference in $Rcr3^{esc}$ (Fig. 1A) may result in activation of an Avr2-independent response upon binding to Cf-2.

With the recent isolation of the Avr2 gene (*28*), it will be possible to determine whether the Avr2, Rcr3, and Cf-2 proteins can interact. This should further increase our understanding of the molecular mechanism of ligand perception by this unique class of R proteins.

### References and Notes


1. J. L. Dangl, J. D. G. Jones, *Nature* **411**, 826 (2001).
2. M. S. Dixon, C. Golstein, C. M. Thomas, E. A. van der Biezen, J. D. G. Jones, *Proc. Natl. Acad. Sci. U.S.A.* **97**, 8807 (2000).
3. M. H. A. J. Joosten, P. J. G. M. de Wit, *Annu. Rev. Phythopathol.* **37**, 335 (1999).
4. T. Romeis, A. Ludwig, R. Martin, J. D. G. Jones, *EMBO J.* **20**, 5556 (2001).
5. M. S. Dixon, K. Hatzixanthis, D. A. Jones, K. Harrison, J. D. G. Jones, *Plant Cell* **10**, 1915 (1998).
6. Details of *Rcr3* cloning and characterization are available on *Science* online at www.sciencemag.org/cgi/content/full/296/5568/744/DC1. The GenBank accession numbers for $Rcr3^{pim}$, $Rcr3^{esc}$, and $Rcr3^{pen}$ (from *L. pennelli*) are AF493232, AF493234, and AF493233, respectively.
7. Single-letter abbreviations for the amino acid residues are as follows: A, Ala; C, Cys; D, Asp; E, Glu; F, Phe; G, Gly; H, His; I, Ile; K, Lys; L, Leu; M, Met; N, Asn; P, Pro; Q, Gln; R, Arg; S, Ser; T, Thr; V, Val; W, Trp; and Y, Tyr.
8. P. J. G. M. de Wit, M. B. Buurlage, K. E. Hammond, *Physiol. Mol. Plant Pathol.* **29**, 159 (1986).
9. A. N. Langford, *Can. J. Res.* (C) **26**, 35 (1948).
10. Clone p28L2 contains $Rcr3^{esc}$, expressed from its native promoter, from the *L. esculentum* cultivar Mogeor.
11. S. Tang, thesis, University of East Anglia (1998).
12. To determine whether *Cf-2/9* and *pCf-9:Cf-2* required *Rcr3* for resistance to *C. fulvum*, transgenic plants were crossed to Cf2 Rcr3-2. Kanamycin-resistant $F_2$ seedlings segregated 3:1 for resistance to *C. fulvum* race 5.
13. M. S. Dixon *et al.*, *Cell* **84**, 451 (1996).
14. To determine whether autonecrosis is $Rcr3^{esc}$-dependent, a *pCf-9:Cf-2* transgenic line was intercrossed with the Cf2 rcr3-2 line. Kanamycin-resistant $F_2$ progeny segregated 19 autonecrotic to 5 wild type ($\chi^2$= 0.22 for a 3:1 ratio). Sequence analysis of asymptomatic plants revealed they were homozygous for the *rcr3-2* mutant allele.
15. *Cf-9* clones were five times more abundant in a cDNA library made from a Cf2/Cf9 line.
16. M. R. Groves *et al.*, *Structure* **4**, 1193 (1996).
17. Details of *Rcr3* epitope tagging and transient expression are available on *Science* Online at www.sciencemag.org/cgi/content/full/296/5568/744/DC1. Various tags for immunodetection were used, including His, His-HA, and HA.
18. To control for protein in the intercellular fluid originating from broken cells, a Western blot was probed with antibodies against AtPhos43, a cytoplasmic *A. thaliana* protein [S. Peck *et al.*, *Plant Cell* **13**, 1467 (2001)].
19. D. Michaud, L. Faye, S. Yelle, *Electrophoresis* **14**, 94 (1993).
20. A. Minami, H. Fukuda, *Plant Cell Physiol.* **36**, 1599 (1995).
21. M. Solomon, B. Belenghi, M. Delledonne, E. Menachem, A. Levine, *Plant Cell* **11**, 431 (1999).
22. M. Estelle, *Curr. Opin. Plant Biol.* **4**, 254 (2001).
23. T. Pechan *et al.*, *Plant Cell* **12**, 1031 (2000).
24. E. K. LeMosy, Y.-Q. Tan, C. Hashimoto, *Proc. Natl. Acad. Sci. U.S.A.* **98**, 5055 (2001).
25. E. A. Levashina *et al.*, *Science* **285**, 1917 (1999).
26. J. Li, K. A. Lease, F. E. Tax, J. C. Walker, *Proc. Natl. Acad. Sci. U.S.A.* **98**, 5916 (2001).
27. J. Vervoort *et al.*, *FEBS Lett.* **404**, 153 (1997).
28. R. Luderer, F. L. W. Takken, P. J. G. M. de Wit, M. H. A. J. Joosten, in preparation.


29. We thank members of the Jones' laboratory and C. Dean for useful discussions, S. Perkins and J. Campling for horticultural service, M. Weaver for binary vector plasmids, O. Voinnet and D. Baulcombe for viral anti-silencing vectors and S. Peck and F. Meins for AtPhos43 antibody. J.K. was supported by an EMBO long-term fellowship. M.D. was supported by Biotechnology and Biological Sciences Research Council grant 208/A06586. The Sainsbury Laboratory is supported by the Gatsby Charitable Foundation.

21 December 2001; accepted 18 March 2002


# A Role for Skin γδ T Cells in Wound Repair


**Julie Jameson,[1] Karen Ugarte,[1] Nicole Chen,[1] Pia Yachi,[1] Elaine Fuchs,[2] Richard Boismenu,[1] Wendy L. Havran[1]***



**γδ T cell receptor–bearing dendritic epidermal T cells (DETCs) found in murine skin recognize antigen expressed by damaged or stressed keratinocytes. Activated DETCs produce keratinocyte growth factors (KGFs) and chemokines, raising the possibility that DETCs play a role in tissue repair. We performed wound healing studies and found defects in keratinocyte proliferation and tissue reepithelialization in the absence of wild-type DETCs. In vitro skin organ culture studies demonstrated that adding DETCs or recombinant KGF restored normal wound healing in γδ DETC-deficient skin. We propose that DETCs recognize antigen expressed by injured keratinocytes and produce factors that directly affect wound repair.**


γδ T cells compose a major T cell component in epithelial tissues (*1*, *2*). The tight correlation between T cell receptor (TCR) V gene segment usage and tissue localization suggests a highly specialized function. γδ TCR-bearing DETCs found in murine skin produce cytokines and proliferate in response to damaged or stressed keratinocytes (*3*), indicating a functional interaction between these two neighboring cell types in vivo. DETCs produce KGF-1, also called fibroblast growth factor-7 (FGF-7), following stimulation through the γδ TCR (*4*). Both FGF-7 and KGF-2 (FGF-10) bind the FGFR2-IIIb receptor and have been implicated in wound healing (*5*–*15*). To directly test the potential role of γδ T cells in wound repair, we set up wound healing studies in mice lacking γδ DETCs.

Location, morphology, and density of DETCs were evaluated after wounding of C57BL/6 mouse ear skin (*16*) (Fig. 1, A through C). Twenty-four to 48 hours after full-thickness wounding, DETCs located around the wound exhibited a change in morphology characterized


[1]Department of Immunology, The Scripps Research Institute, La Jolla, CA 92037, USA. [2]Department of Molecular Genetics and Cell Biology, Howard Hughes Medical Institute, The University of Chicago, Chicago, IL 60637, USA.

*To whom correspondence should be addressed. E-mail: havran@scripps.edu